

Transport of African Swine Fever Virus from Assembly Sites to the Plasma Membrane Is Dependent on Microtubules and Conventional Kinesin

Nolwenn Jouvenet,¹ Paul Monaghan,¹ Michael Way,² and Thomas Wileman^{1*}

Department of Immunology and Pathology, Pirbright Laboratories, Institute for Animal Health, Woking, Surrey GU24 0NF,¹ and Cell Motility Laboratory, Cancer Research UK, Lincoln's Inn Fields Laboratories, London WC2A 3PX,² United Kingdom

Received 21 November 2003/Accepted 6 April 2004

African swine fever virus (ASFV) is a large DNA virus that assembles in perinuclear viral factories located close to the microtubule organizing center. In this study, we have investigated the mechanism by which ASFV reaches the cell surface from the site of assembly. Immunofluorescence microscopy revealed that at 16 h postinfection, mature virions were aligned along microtubules. Furthermore, virus movement to the cell periphery was inhibited when microtubules were depolymerized by nocodazole. In addition, ASFV infection resulted in the increased acetylation of microtubules as well as their protection against depolymerization by nocodazole. Immunofluorescence microscopy showed that conventional kinesin was recruited to virus factories and to a large fraction of virus particles in the cytoplasm. Consistent with a role for conventional kinesin during ASFV egress to the cell periphery, overexpression of the cargo-binding domain of the kinesin light chain severely inhibited the movement of particles to the plasma membrane. Based on our observations, we propose that ASFV is recognized as cargo by conventional kinesin and uses this plus-end microtubule motor to move from perinuclear assembly sites to the plasma membrane.

Viral replication and assembly often take place in specialized structures located in the nucleus or in the perinuclear cytoplasm. These specialized sites, called viral inclusions or virus factories, provide a focal point for the replication of virus genomes and the recruitment of structural proteins. Recent work has focused on understanding how viruses travel to, and from, these specialized sites during their infectious cycle. One common viral strategy uses microtubules for directed long-range transport of virus components inside cells (44, 52, 54). Directional movement along microtubules is mediated by motor proteins which hydrolyze ATP to induce the conformational changes necessary to move cargoes along microtubules (30, 62).

Movement of cellular materials towards the microtubule organizing center (MTOC) (retrograde transport) usually requires the minus-end directed microtubule motor dynein (62). The transport of cargoes by dynein requires association with dynactin, a heterooligomeric complex of at least nine different polypeptides. This has been demonstrated experimentally by the overexpression of the p50-dynactin subunit of the dynactin complex, which dissociates the dynactin complex and severely affects vesicular trafficking and organelle distribution (10). Importantly, retrograde transport of several unrelated viruses, such as herpes simplex virus type 1 (HSV-1), adenovirus, vaccinia virus (VV), parvovirus, and human immunodeficiency virus type 1 is inhibited when the dynactin complex is

dissociated, suggesting that dynein is required for inward transport of these viruses (18, 38, 43, 57, 59).

The movement along microtubules, from the MTOC towards the plasma membrane (anterograde transport), involves the kinesin family of motor proteins (62). Conventional kinesin is a heterotetramer consisting of two heavy and two light chains (63). The N terminus of each heavy chain contains a motor domain that binds microtubules. The N-terminal domain of the light chain binds the heavy chain, and the C-terminal domain consists of six tetratricopeptide (TPR) motifs that can mediate interaction with cellular cargoes (23, 62). Interestingly, recent reports have revealed a link between conventional kinesin and the movement of HSV-1 and VV in cells. During the vaccinia life cycle, the intracellular mature virus (IMV) form leaves the virus factory and travels to the Golgi, where it is wrapped by the *trans*-Golgi network (TGN) (55). The movement of the IMV from the factory to the TGN requires microtubules (51), but the nature of the motor involved in this traffic is unknown. After envelopment by the TGN, the intracellular enveloped virus (IEV) recruits conventional kinesin and moves in a microtubule-dependent fashion to the plasma membrane (28, 45, 67). An involvement of conventional kinesin in HSV-1 anterograde transport is consistent with both the speed and type of movement exhibited by virus particles in the axon (53). In fact, conventional kinesin is recruited to the surface of unenveloped HSV-1 in human fetal axons, where it may bind tegument protein US11 (17). The precise site where HSV-1 becomes recognized as a cargo for kinesin motors has not, however, been resolved.

African swine fever virus (ASFV) is a very large enveloped DNA virus and has been described as the missing evolutionary link between the *Poxviridae* and the *Iridoviridae* (50). In common with poxviruses and iridoviruses, ASFV is assembled in

* Corresponding author. Mailing address: Department of Immunology and Pathology, Institute for Animal Health, Pirbright Laboratories, Ash Road, Woking, Surrey GU24 0NF, United Kingdom. Phone: 44 1483 232441. Fax: 44 1483 232448. E-mail: thomas.wileman@bbsrc.ac.uk.

virus factories located close to the MTOC (26, 39, 43). Assembly is initiated by the recruitment of structural proteins from the cytosol into the factory where they bind membrane structures thought to be derived from the endoplasmic reticulum (ER) (4, 14, 15, 27, 49). The progressive assembly of capsid and matrix proteins on the cytoplasmic face of these membranes leads to the production of fully assembled icosahedral particles that appear as 200-nm hexagons in cross-sections taken through virus assembly sites (49). Following assembly, mature ASFV particles leave the factory, move through the cytoplasm, and are eventually released from the cell by budding through the plasma membrane (6). Early studies have shown that ASFV particles associate with microtubules *in vitro* (16), and recent works suggest that retrograde dynein-dependent microtubule transport is required for the inward movement of the virus (3, 26). Given the observations on VV and HSV-1 anterograde transport, we examined the role of microtubules and conventional kinesin in the movement of ASFV from sites of assembly to the plasma membrane. We found that mature ASFV particles align along microtubules and that their movement to the cell periphery is dependent on microtubules. Conventional kinesin was found to be recruited to both viral factories and virions. Consistent with a role for conventional kinesin during ASFV egress to the cell periphery, overexpression of the cargo-binding domain of the kinesin light chain severely inhibited the movement of particles to the plasma membrane.

MATERIALS AND METHODS

Cell culture, virus, and drug treatments. Vero cells (ECACC 84113001) were obtained from the European Collection of Animal Cell Cultures (Porton Down, United Kingdom). Cells were grown at 37°C in HEPES-Dulbecco's modified Eagle medium supplemented with 10% fetal calf serum and infected with the tissue culture-adapted Ba71v strain of ASFV (12). The Ba71v stock used in this study had a titer of 1.4×10^7 PFU/ml. Infections were allowed to progress for the indicated time. Nocodazole and paclitaxel (Sigma-Aldrich, St. Louis, Mo.) were dissolved in dimethyl sulfoxide (DMSO) and used at a concentration of 10 µg/ml and 10 µM, respectively. Cytosine α -D-arabino-furanoside (Ara-C) (Sigma) was used at a concentration of 50 µg/ml at 2 h postinfection, a time calculated to allow viral attachment and entry.

Antibodies. Antibody 4H3, specific for the major capsid protein p73 of ASFV, has been previously described (14). SB11 was obtained from rabbits immunized with the synthetic peptide NSPIQYLKEDSRDRTSIGSLYDE, which corresponds to amino acids 5 to 27 of the viral protein pE120R. The specificity of SB11 was characterized by immunoprecipitation, Western blotting, and immunofluorescence analysis on ASFV-infected Vero cells (data not shown). The anti-pE120R serum was used at a dilution of 1:500 for immunofluorescence. The anti-pJ13L rabbit antiserum has been previously described (58) and was used at a dilution of 1:500. C18, the mouse monoclonal antibody specific for the ASFV early protein p30 has been described previously (1). Antibody 63-90, directed against the light chain of kinesin, was provided by Scott Brady (University of Texas, Dallas) (56). Monoclonal antibodies against α -tubulin and acetylated- α -tubulin (Sigma) were used at dilutions of 1:2,000 and 1:200, respectively. Goat anti-mouse and anti-rabbit Alexa Fluor 488 (green) and Alexa Fluor 594 and 568 (red) conjugates were used at 1:500 (Molecular Probes, Leiden, The Netherlands). Goat anti-rabbit and anti-mouse horseradish peroxidase conjugates were purchased from Promega, Southampton, United Kingdom.

pEL expression clones. The pEL-GFP-TPR construct has been previously described (45). pET-21a-5AR was provided by Manuel Borca (Plum Island Animal Disease Center, New York, N.Y.) (8) and was used as a template to amplify the 5AR open reading frame by using the primers 5'-GGGGCGGCCGCTCGACAAAAAAG-3' and 5'-TTTGAATTCTTAATTTAATATATC-3'. The resulting PCR products were cloned into the NotI-EcoRI sites of the expression vector pEL-GFP (20) to generate 5AR tagged at the N terminus with green fluorescent protein (GFP-5AR). The fidelity of the clone was confirmed by sequencing.

Transfection, pEL driven expression, and fluorescence microscopy. Vero cells were grown to 70% confluency and were transiently transfected by using a liposomal Transfast transfection system (Promega). For pEL-driven expression, cells were transfected 2 h prior to infection. Cells were either fixed in 4% paraformaldehyde or in 4% paraformaldehyde-PHEM (60 mM PIPES, 25 mM HEPES, 10 mM EGTA, 1 mM MgCl₂, pH 7.4) for 10 min and then permeabilized in 0.1% Triton X-100 for 15 min. Samples were blocked in 0.5% bovine serum albumin-phosphate-buffered saline for 30 min and incubated with the first antibody in the same solution for 1 h. Cells were incubated with the Alexa Fluor 488- or 594-conjugated secondary antibody for 60 min before being stained for 5 min with 1:20,000 4',6-diamidino-2-phenylindole (DAPI) (Sigma). Preparations were viewed either with a Leica SP2 confocal microscope or with a Nikon E800 microscope connected to a Hamamatsu C-4746A CCD camera. Images were processed by using the Improvision Openlab 2.1.3 software (Improvision, Coventry, United Kingdom).

Immunoprecipitation and Western blot analyses. Infected cells were labeled with [³⁵S]methionine-cysteine Promix (Amersham, Little Chalfont, United Kingdom), and proteins were immunoprecipitated as described previously (15). Proteins were resolved by sodium dodecyl sulfate-polyacrylamide gel electrophoresis and transferred onto Protan BA85 nitrocellulose membranes (Schleicher and Schuell, Dassel, Germany) as described previously (49). Protein extracts were quantified with the BCA kit (Pierce Chemical Co., Rockford, Ill.), and samples were equally loaded.

Preparation of electron microscopy (EM) samples. Vero cells were plated onto Thermanox coverslips and infected with ASFV for the indicated time. They were fixed *in situ* in 2% glutaraldehyde in 0.05 M phosphate buffer (pH 7.2 to 7.4, osmotic pressure adjusted to 350 mosmol with sucrose) for a minimum of 2 h. Samples were post-fixed in 1% osmium tetroxide in phosphate buffer for a minimum of 4 h, dehydrated through a graded series of ethanols, and embedded in agar 100 resin (Agar Scientific, Stanstead, United Kingdom). After overnight polymerization at 60°C, the coverslips were peeled from the resin block leaving the cells embedded in the resin. Sections were cut parallel to the coverslip surface on a Diatome diamond knife (Leica Microsystems, London, United Kingdom) and contrasted with uranyl acetate and lead citrate with an EMstain (Leica). They were imaged in an FEI Tecnai 12 at 100 kV.

RESULTS

ASFV spread to the cell surface requires microtubules. To examine the relationship between ASFV and microtubules, we performed immunofluorescence analysis of infected cells at 16 h postinfection (hpi) by using antibodies against the late viral protein pE120R and α -tubulin (Fig. 1). Viral factories were located by extranuclear DAPI staining of viral DNA. Viral particles were concentrated in viral factories but also observed throughout the cytoplasm (Fig. 1A). Higher magnification analyses revealed a colocalization of cytoplasmic particles with microtubules (Fig. 1C and D).

To ensure that the pE120R antibody was recognizing newly synthesized viruses, rather than viruses entering cells, immunofluorescence analyses of infected cells were performed at different times postinfection, as well as in the presence of Ara-C, a drug that inhibits late gene expression (Fig. 2). Cells at early stages of infection were identified by positive staining for the nonstructural ASFV protein p30, which is expressed as early as 2 hpi (1). At 4 and 8 hpi, cells positive for p30 were pE120R negative (Fig. 2), showing that viruses entering the cell to initiate the infection are present at very low levels, or that disassembly following entry results in the loss of immunostaining of the virus by antibodies recognizing pE120R. The lack of immunostaining for pE120R observed in the presence of Ara-C confirmed that incoming viruses were not detected by the pE120R antibody. Similar results were obtained with antibody directed against the p73 capsid protein (data not shown).

In a typical experiment, more than 80% of newly assembled viruses ($n = 358$) were associated with a microtubule (Fig. 1).

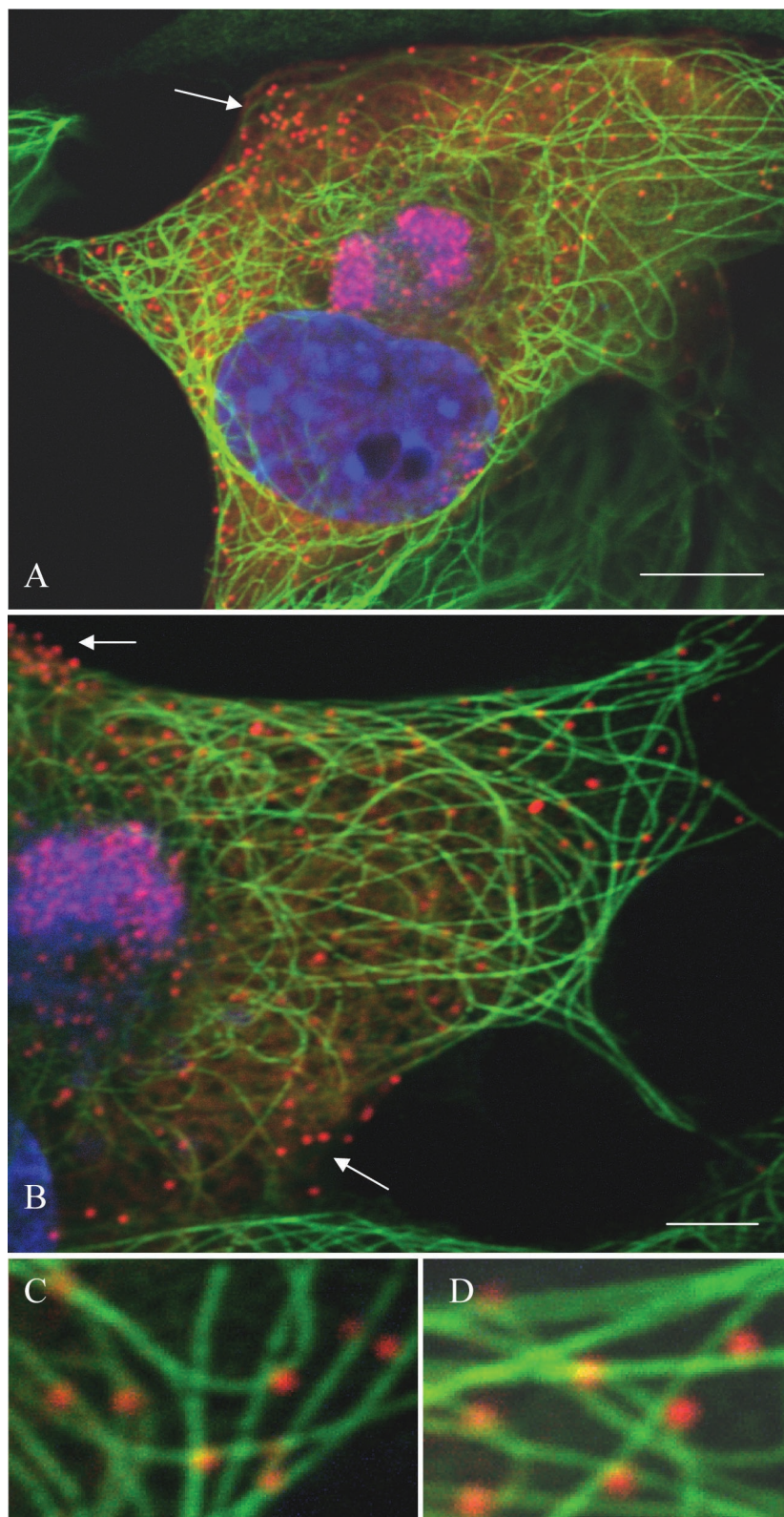


FIG. 1. ASFV particles associate with microtubules. Vero cells were infected with the Ba71v strain of ASFV and fixed at 16 hpi. Samples were incubated with a rabbit antiserum raised against the late ASFV structural protein pE120R (red) and a mouse antibody against α -tubulin (green). Viral DNA and cellular DNA were labeled with DAPI (blue). Images shown have been collected sequentially with a confocal laser scanning microscope and merged. The arrows indicate viral particles that do not align with microtubules. Panels C and D show enlarged views of parts of B. Scale bars, 8 μ m (A) and 4 μ m (B).

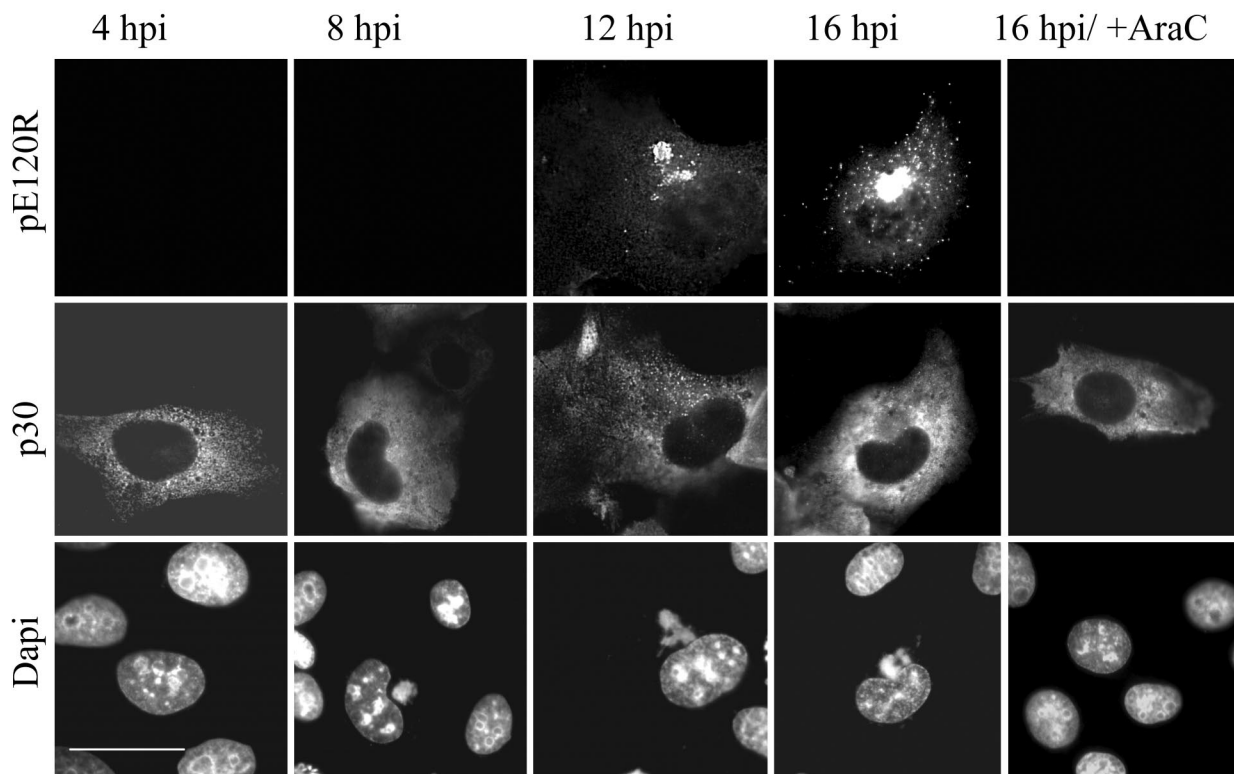


FIG. 2. The anti-pE120R antibody recognizes newly assembled virions. Vero cells were infected with the Ba71v strain of ASFV, fixed at the indicated time, and processed for immunofluorescence. Samples were incubated with a rabbit antiserum raised against the late ASFV structural protein pE120R (top panels) and a mouse antibody against the early viral protein p30 (middle panels). Viral DNA and cellular DNA were labeled with DAPI (bottom panels). The ASFV structural protein pE120R is not detected until 12 hpi or not at all in the presence of Ara-C, an inhibitor of late gene expression. Scale bar, 20 μ m.

The remaining cytoplasmic particles were in the peripheral regions of the cytoplasm, very close to the cell surface (Fig. 1A and B, arrows). Interestingly, the tubulin signal was excluded from the core of the replication site, but some microtubule filaments were clearly in contact with the edge of the factory (Fig. 1B). To determine whether microtubules were required for movement of ASFV into the cytoplasm, infected cells were incubated with the microtubule-destabilizing agent nocodazole or the microtubule-stabilizing drug paclitaxel. The drugs were added at 12 hpi, a time when newly assembled virions start to leave the viral factory (Fig. 2). Cells were fixed at 16 h and analyzed by immunofluorescence (Fig. 3A). Over 200 infected cells were examined, and viral dispersion was quantified by counting individual mature particles located outside the factory. The depolymerization of microtubules at 12 hpi resulted in approximately 88% inhibition of ASFV dispersion from the assembly sites (Fig. 3B), indicating that an intact microtubule network was required for ASFV movement from the factory to the plasma membrane. In contrast, when microtubules were stabilized with paclitaxel, there was no effect on viral transport (Fig. 3B), suggesting that movement of ASFV from the factories does not require dynamic microtubules.

Addition of nocodazole at 12 hpi does not affect ASFV replication or assembly. It was important to establish that the depolymerization of microtubules by the addition of nocodazole at 12 hpi was affecting the movement of mature virus from assembly sites to the plasma membrane rather than blocking

the supply of viral proteins important for virus replication and/or assembly. The experiment above was repeated, and the effects of nocodazole on the synthesis of two late viral proteins that are recruited into virus factories were tested. The expression of the main ASFV capsid protein, p73, was assessed by immunoprecipitation from lysates taken from cells pulse-labeled with [³⁵S]methionine and cysteine 30 min after incubation with the drugs for 3.5 h (Fig. 4A, top panel). The level of expression of pJ13L, a late membrane protein (46), was examined by Western blotting (Fig. 4A, bottom panel). The results show that nocodazole did not affect the expression of these two late proteins.

EM was used to further examine the effects of nocodazole on viral morphology. Figure 4B compares the virus factories in control cells with those incubated with nocodazole. The morphology of ASFV particles, which appear as hexagons in cross-section, was unaffected by nocodazole (Fig. 4B, panels i and ii). Fully assembled particles appeared as electron-dense hexagons on the images (Fig. 4B, arrows). Interestingly, factories formed in the presence of nocodazole contained greater numbers than control cells of these mature virions (Fig. 4B, panels iii and iv). Taken together, the results suggest that ASFV replicates and assembles normally when nocodazole is added at 12 hpi. However, addition of the drug at 12 hpi prevents the spreading of ASFV particles from the factories to the plasma membrane.

ASFV infection increases the stability of microtubules. Close inspection of infected cells incubated with nocodazole

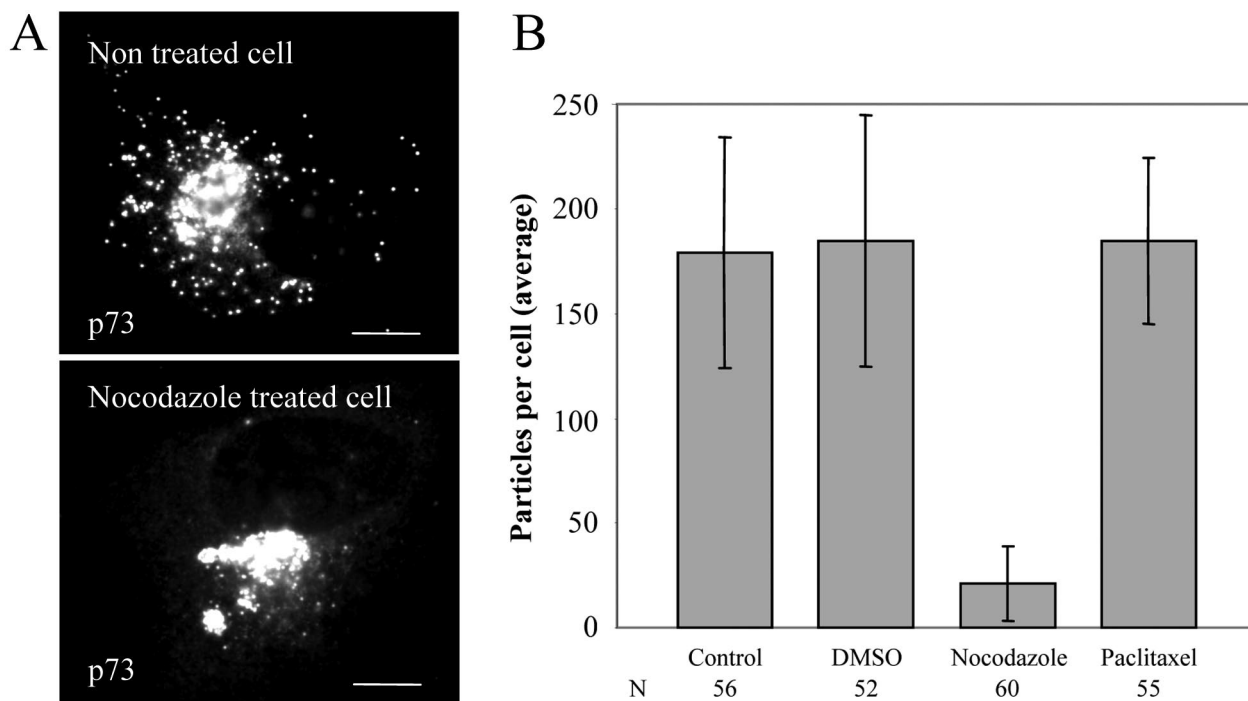


FIG. 3. Effect of nocodazole and paclitaxel on movement of ASFV into the cytosol. Vero cells were infected with the Ba71v strain of ASFV. Nocodazole, paclitaxel, or control (DMSO) was added at 12 hpi, and cells were incubated for a further 4 h prior to fixation and processing for immunofluorescence. Virions were located by immunofluorescence staining by using an antibody specific for the main capsid protein p73. (A) Immunofluorescence images show viral dispersion in a control cell and a cell incubated with nocodazole. Scale bar, 8 μ m. (B) Cells were examined by microscopy as described above, and viral dispersion was quantified by counting individual particles located outside the factory. Results are presented as the average number of virions present in the cytoplasm per cell. Error bars indicate the standard deviations of the means. N, number of cells evaluated.

identified a subpopulation of microtubules that were protected from depolymerization by the drug (Fig. 5, arrow). These appeared as bright fluorescent tracks within a strong diffuse fluorescence signal provided by depolymerized tubulin. The numbers of microtubules stabilized by the infection varied from cell to cell; however, in cells negative for viral antigen, microtubules were totally depolymerized (Fig. 5, star). Figure 5 compares the distribution of ASFV particles in cells with low or high numbers of stabilized microtubules. Interestingly, there was a positive correlation between the number of stabilized microtubules and the number of viral particles in the cytoplasm of nocodazole-treated cells (compare top and bottom panels). The analysis was repeated by using an antibody against acetylated tubulin. Although the role of acetylated tubulin is not clear, it is known to correspond to stable but not dynamic microtubules (42, 48). The level of acetylated tubulin was clearly higher in pE120R-positive cells (Fig. 6A, arrow) than in pE120R-negative ones (Fig. 6A, stars). Acetylated tubulin appeared to be concentrated around the virus factory (Fig. 6A). The acetylation of tubulin was also analyzed by Western blotting of total cell lysates collected at different times postinfection. The level of acetylated tubulin increased at around 12 hpi (Fig. 6B, top panel), a time that correlated with the start of ASFV movement from the virus factory (see Fig. 2). The Western blots also showed that the overall level of α -tubulin stayed constant following infection (Fig. 6B, bottom panel). The results reflected the increased acetylation of tubulin rather than

an increase in the synthesis of tubulin in the infected cells. Importantly, immunofluorescence preparations viewed at higher magnification showed that many viral particles were associated with acetylated microtubules (Fig. 6C), suggesting a link between acetylation, stabilization, and virus movement into the cytoplasm.

Conventional kinesin light chain is recruited into factories. To address the possibility that conventional kinesin was involved in ASFV anterograde transport, infected cells were analyzed by immunofluorescence at 16 hpi by using an antibody specific for the N-terminal domain of conventional kinesin light chain (56). In noninfected cells, the kinesin light-chain antibody produced dot-like staining throughout the cytoplasm. A concentration of kinesin was noticeable at the cell periphery but not around the nucleus (Fig. 7A). In infected cells, the kinesin antibody revealed an intense staining of perinuclear viral factories containing viruses stained with the antibody recognizing pE120R (Fig. 7B). The presence of large numbers of small vesicular structures staining strongly with kinesin throughout the cytoplasm makes colocalization studies difficult. However, the majority of virions located outside the factory appeared yellow when merged with the kinesin signal, suggesting colocalization of kinesin with a large portion of virus particles (Fig. 7B, merge panels).

ASFV factories and virions recruit kinesin light chain via its TPR repeat. The C-terminal tail domain of kinesin heavy chain and the TPR domain of the light chain have been shown to

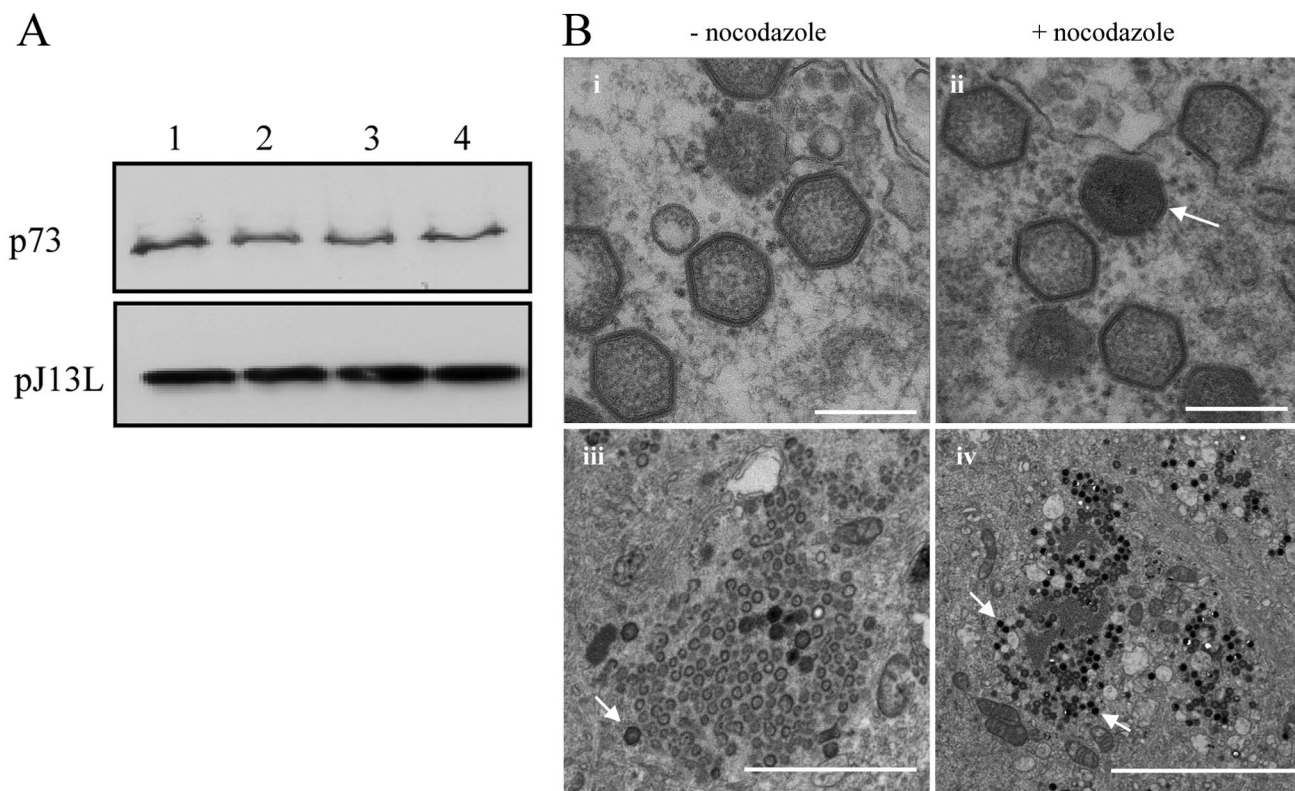


FIG. 4. Effect of nocodazole on ASFV replication and assembly. (A) Effect of nocodazole on synthesis of viral late proteins. Vero cells were infected with ASFV, and nocodazole, paclitaxel, or control (DMSO) was added at 12 hpi. Samples were either labeled with [³⁵S]methionine and cysteine for 30 min and immunoprecipitated 3.5 h later by using antibody specific for p73 (top) or incubated for a further 4 h and assayed for expression of pJ13L by Western blotting (bottom). Lane 1, no additions; lane 2, DMSO control; lane 3, nocodazole; lane 4, paclitaxel. (B) Effect of nocodazole on assembly of ASFV. Vero cells were infected with the Ba71v strain of ASFV. Nocodazole or control (DMSO) was added at 12 hpi, and cells were incubated for a further 4 h prior to processing for EM. Micrographs in frames i and ii show thin-section images of viruses formed in the presence (+) or absence (-) of nocodazole as indicated. Scale bar, 250 nm. Micrographs in frames iii and iv show similar images of virus assembly sites at lower magnification. The arrows indicate fully assembled virions. Scale bars, 2 μm (iii) and 5 μm (iv).

mediate cargo interactions (62). GFP-TPR fusion polypeptides can be used to identify cellular components that are recognized as cargo by kinesin light chain. This method has been used successfully to demonstrate that VV particles recruit conventional kinesin light chain via the TPR domain (45). The same pEL-GFP-TPR probe was expressed in ASFV-infected cells, and the distribution of the GFP signal was analyzed by immunofluorescence at 12 and 16 hpi. Figure 8 shows that the VV EL promoter was recognized by ASFV transcriptional machinery, allowing the GFP-TPR protein to be expressed in infected cells. The top panels of Fig. 8A show two infected cells viewed at 12 hpi. One cell was positive for the late viral antigen p73 (star), and the other cell was negative for p73 (arrow) but nonetheless infected because it expressed the GFP-TPR, suggesting an earlier stage of infection. Significantly, at this early stage, the GFP-TPR signal was distributed throughout the cytoplasm (arrow); in contrast, in the cell expressing p73, the GFP probe was concentrated in the ASFV factory (star). These results demonstrate active recruitment of the GFP-TPR protein to virus assembly sites and confirm the data obtained with the 63-90 antibody (Fig. 7). At 16 hpi, when mature viral particles could be visualized in the cytoplasm, GFP-TPR was still concentrated in the factory but also labeled 100% of cytoplasmic particles (*n* = 231) (Fig. 8A, bottom panels).

ASFV factories contain viruses at various stages of assembly interwoven within a matrix of membranous material derived from the ER (4, 49). To determine which of these structures was labeled by the TPR-probe, the location of the TPR-GFP signal within the virus factory was studied in more detail at 12 hpi. The membranes within the factory were labeled by using antibodies recognizing virally encoded membrane protein pJ13L (46), while virions were labeled with antibodies specific for the major capsid protein p73. The panels in Fig. 8B show that the GFP-TPR signal colocalized with p73 but not with pJ13L, demonstrating that the mature virions, and not the underlying membranous structures, are responsible for recruiting the TPR domain of kinesin light chain.

Anterograde transport of ASFV is dependent on conventional kinesin. During our experiments, we noticed that viral dispersion was impeded in cells expressing high levels of GPP-TPR. The GFP-TPR probe acts as a dominant-negative protein by replacing the N-terminal domain of kinesin light chain, which would normally interact with the kinesin heavy chain, with GFP. The resulting protein can bind cargo via the TPR domain but cannot recruit the heavy chain for transport on microtubules. High levels of TPR-GFP expression would be expected to saturate the binding sites for the endogenous conventional kinesin and, thus, inhibit ASFV transport. To test

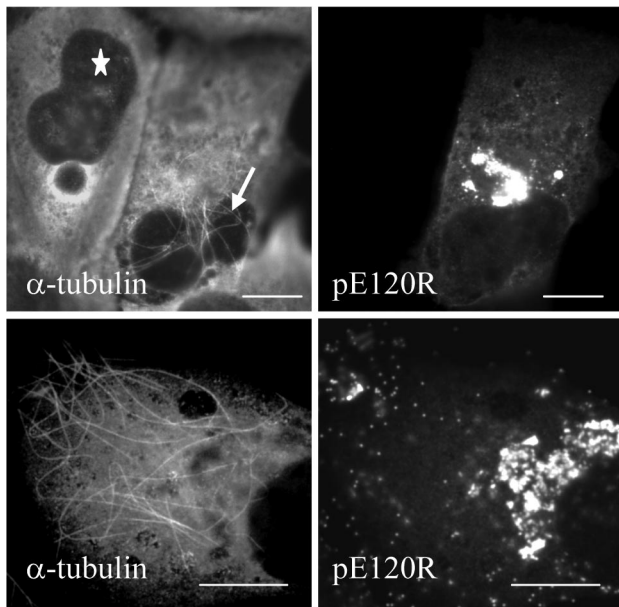


FIG. 5. Microtubules are stabilized in cells infected with ASFV. Vero cells were infected with ASFV, and nocodazole was added at 12 hpi. Cells were incubated for a further 4 h prior to fixation and immunofluorescence microscopy analysis. Infected cells were identified by using a rabbit antiserum raised against the late ASFV structural protein pE120R, and a mouse antibody against α -tubulin was used to label microtubules. The star indicates a pE120R-negative cell, while the arrow indicates stabilized microtubules in a pE120R-positive cell. Scale bar, 8 μ m. The figure compares cells with low (top panel) and high (bottom panels) numbers of stabilized microtubules.

this hypothesis, ASFV dispersion was quantified by counting individual particles located outside the factory in cells expressing high levels of GFP-TPR. The top panels of Fig. 9A compare the distribution of ASFV particles in a cell expressing high levels of the GFP-TPR protein with two neighboring cells negative for GFP-TPR signal. Far fewer viral particles were seen in the cytoplasm of the cell expressing GFP-TPR compared to the two infected but nontransfected cells. The lower panels show a control experiment where a GFP-tagged viral DNA-binding-protein, GFP-5AR, was expressed at similar levels in infected cells. The GFP-5AR protein located to virus factories but did not prevent the dispersion of ASFV particles in the cytoplasm. An analysis of virus distribution is presented graphically in panel B of Fig. 9. High-level expression of TPR-GFP resulted in approximately 97% inhibition of ASFV transport to the plasma membrane. In contrast, high-level expression of GFP-5AR has no effect on viral transport. These data demonstrate that the movement of newly assembled ASFV particles from the factory to the cell surface is dependent on conventional kinesin.

DISCUSSION

This study provides evidence that ASFV anterograde transport requires microtubules and, importantly, implicates conventional kinesin as the motor responsible. Immunofluorescence analyses show that newly assembled viruses were closely aligned with microtubules (Fig. 1) and that ASFV movement

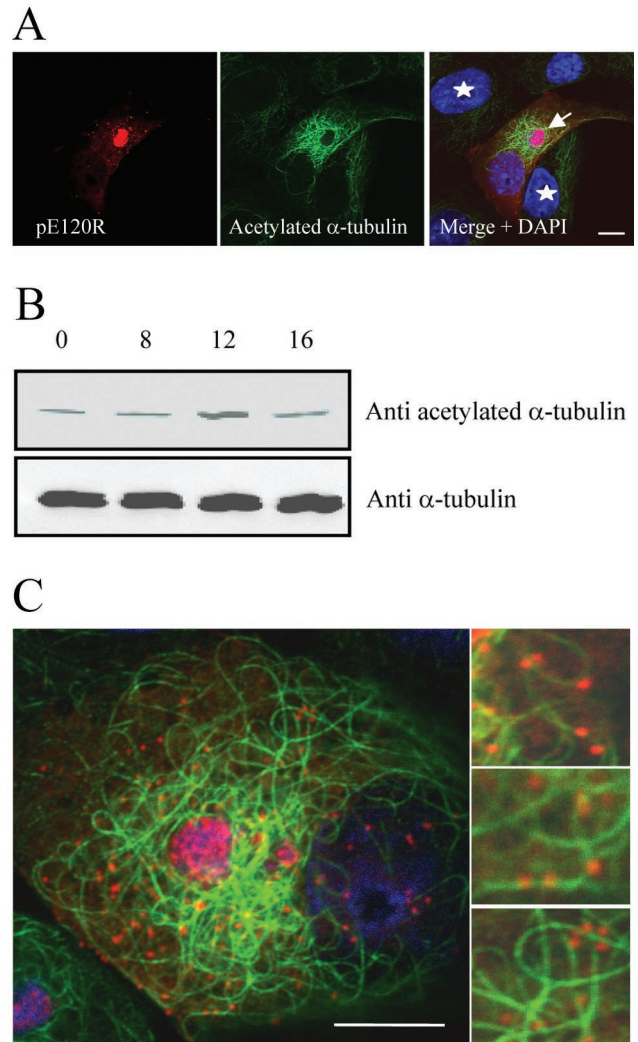


FIG. 6. ASFV infection induces acetylation of microtubules. (A and B) Identification of acetylated tubulin. Panel A shows Vero cells infected with the Ba71v strain of ASFV and fixed at 16 hpi. Samples were incubated with a rabbit antiserum raised against the late ASFV structural protein pE120R (red) and a mouse antibody against acetylated α -tubulin (green). Viral and cellular DNA were labeled with DAPI (blue). Stars indicate cells that are pE120R negative, and the arrow indicates an infected cell. Scale bar, 8 μ m. Panel B shows Vero cells infected with the Ba71v strain of ASFV and lysed at the indicated times. Samples were analyzed by Western blotting with antibodies specific for α -tubulin or acetylated α -tubulin as indicated. (C) ASFV particles associate with acetylated microtubules. Vero cells were infected with ASFV and processed for immunofluorescence at 16 h. Samples were incubated with a rabbit antiserum raised against structural protein pE120R (red) and a mouse antibody against acetylated α -tubulin (green). Viral DNA and cellular DNA were labeled with DAPI (blue). Images shown were collected sequentially with a confocal laser scanning microscope and merged. Right panels are enlarged views of parts of the left image. Scale bar, 8 μ m.

from the sites of assembly to the plasma membrane was markedly inhibited when microtubules were depolymerized by nocodazole (Fig. 3). The alignment of ASFV with microtubules in cells is consistent with previous work showing the binding of ASFV with microtubules *in vitro* (16). Previous studies have also implicated a role for microtubules during virus exit by

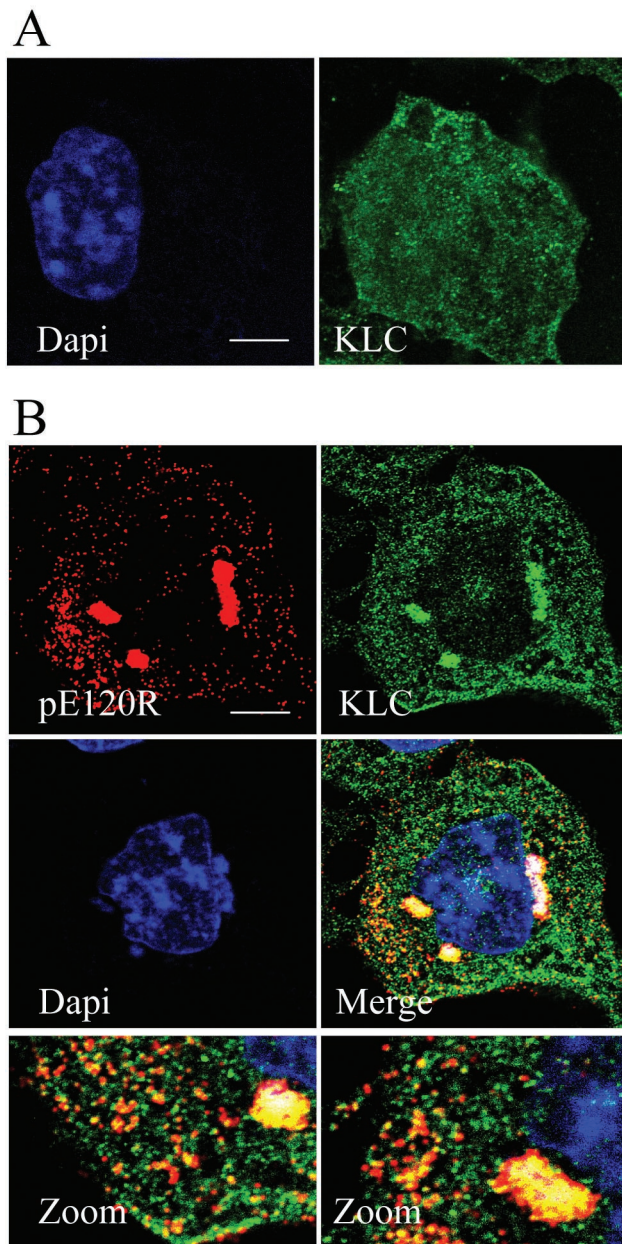


FIG. 7. Conventional kinesin is recruited into ASFV assembly sites. (A) Distribution of kinesin light chain in noninfected cells. Noninfected Vero cells were fixed and processed for immunofluorescence by using the mouse kinesin light-chain antibody 63-90 (green). Cellular DNA was labeled with DAPI (blue). (B) Distribution of kinesin light chain in ASFV-infected cells. Vero cells were infected with the Ba71v strain of ASFV, fixed at 16 hpi, and processed for immunofluorescence. Rabbit antiserum raised against the structural protein pE120R was used to locate virus particles (red), and conventional kinesin light chain was identified by using the mouse antibody 63-90 (green). Viral DNA and cellular DNA were labeled with DAPI (blue). The bottom panels are enlarged views of the merge image. Scale bar, 8 μ m.

showing that the depolymerization of microtubules early during infection reduces yields of ASFV (13). The early depolymerization of microtubules, however, slows the formation of virus assembly sites and inhibits virus replication (3, 13, 26). It is possible that the reduced virus yield observed in these earlier

studies results from a reduced production of viruses in cells rather than from a requirement for intact microtubules during virus egress. In this present study, nocodazole was added 12 h after infection, allowing late gene expression and virus assembly to occur before depolymerization of the microtubules (Fig. 4). Incubation with nocodazole for a further 4 h did not affect the synthesis of two late structural proteins or the morphology of viruses in virus assembly sites (Fig. 4). The major effect of nocodazole was to markedly reduce the number of mature viruses en route to the plasma membrane and to increase their number in assembly sites (Fig. 3 and 4). The results suggest that once viruses are assembled, they need intact microtubules to leave the virus factory.

Interestingly, nocodazole does not block all ASFV movement, suggesting that the dependence on microtubules is not absolute (Fig. 3B). The same observation holds for the retrograde transport of adeno-associated virus, HSV-1, retroviruses (52), and polyomavirus (22). The actin cytoskeleton might be considered as an alternative pathway for viral retrograde transport, and it appears to be used as such by a baculovirus (34). However, for adenovirus the movement seen in nocodazole-treated cells is not the result of actin-based transport because the simultaneous treatment of cells with nocodazole and an actin-disruptive agent does not block viral transport (24). One attractive explanation to account for nocodazole-independent movement of ASFV particles is our observation that ASFV infection induces the stabilization of some microtubules against exposure to nocodazole (Fig. 5). These hyperacetylated microtubules, which are associated with viral particles (Fig. 6), may explain how 12% of viral particles reached the cell periphery in the presence of nocodazole (Fig. 3).

ASFV is not the only virus to stabilize the microtubule network. The reovirus μ 2 protein induces changes in microtubule organization similar to those seen in cells overexpressing microtubule-associated-proteins (41). The Vp22 tegument protein of HSV-1 colocalizes with microtubules in infected cells and stabilizes them against exposure to nocodazole when expressed alone (19). VV infection also stabilizes the microtubule network, and viral particles associate with a subpopulation of acetylated microtubules (43). Taken together, these studies suggest that microtubule stabilization during viral infection may be important for the movement of viruses, or virus-induced structures, in cells. In vitro studies have shown that conventional kinesin binds with higher affinity to polyglutamylated and detyrosinated tubulin (32, 35, 36). If this were also true for acetylated tubulin, then ASFV would not only stabilize the microtubules but also enhance the binding of kinesin; both would facilitate transport of the virus from factories to the cell surface.

Immunostaining showed that kinesin light chain was associated with virus particles at the site of assembly in perinuclear factories and with a large portion of particles in the cytosol (Fig. 7). However, the presence of many viral particles and small vesicular structures stained with the kinesin antibody throughout the cytoplasm makes colocalization studies difficult (Fig. 7B). A number of virions lacked kinesin staining, particularly those outside the cell or near the cell surface. It is possible that kinesin dissociates from particles at some point after they leave the virus factory. The lack of complete colocalization between kinesin light chain and virions could also be

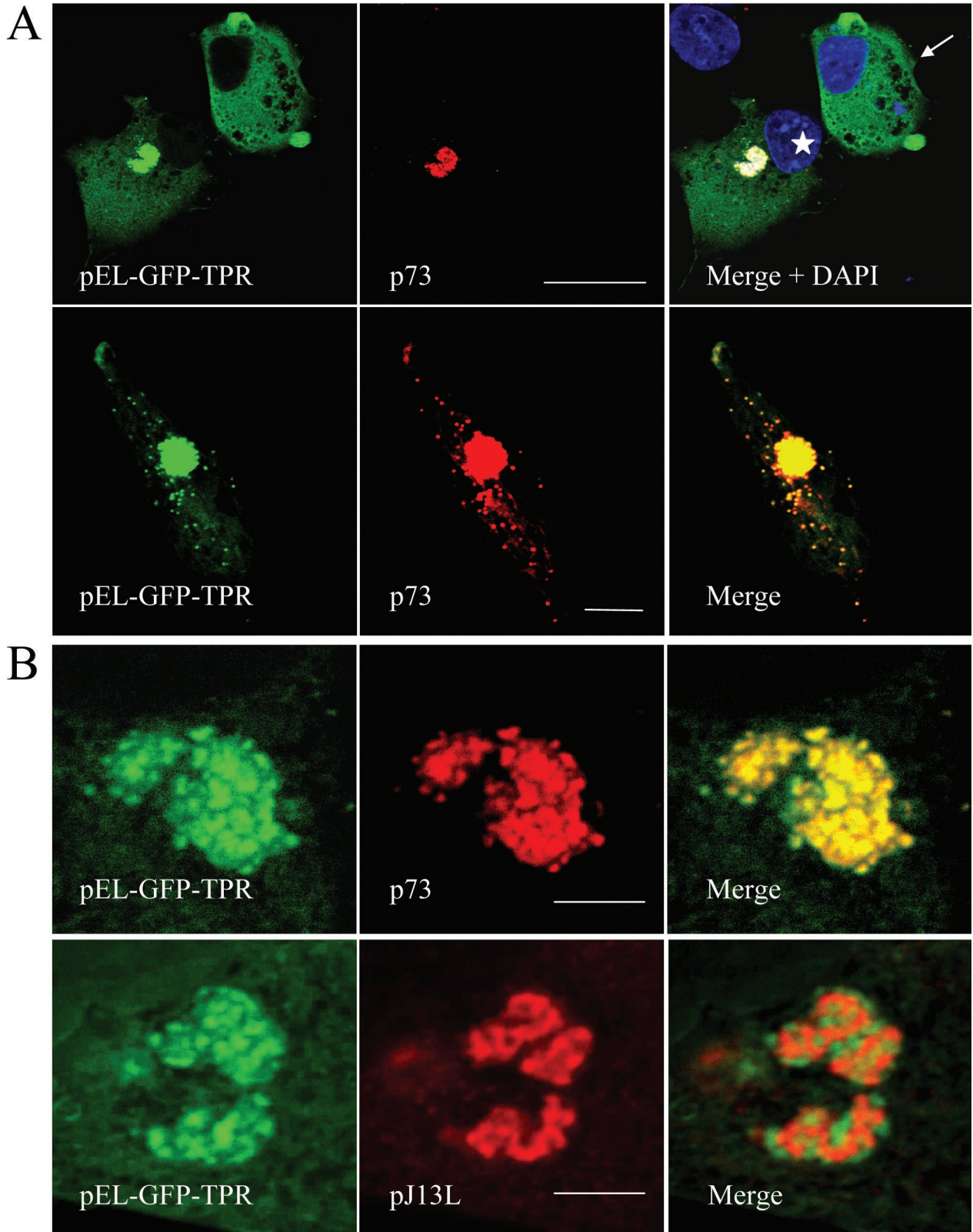


FIG. 8. ASFV particles bind the TPR domain of kinesin light chain. Vero cells were transfected with pEL-GFP-TPR and infected with ASFV 2 h later. Cells were processed for immunofluorescence by using antibodies specific for the late viral protein p73 (red) at the times indicated below. The subcellular localization of the TPR domain of kinesin light chain was monitored by the intrinsic fluorescence of GFP-TPR (green). (A) In the top gallery cells were fixed at 12 h and a view was chosen to show the distribution of GFP-TPR in the presence (star) or absence (arrow) of p73. Viral DNA and cellular DNA were labeled with DAPI (blue). Scale bar, 20 μm . In the bottom gallery cells were fixed at 16 h, and cells expressing low levels of GFP-TPR were selected to show the location of GFP-TPR in cells where virions were located outside the factory. Scale bar, 8 μm . (B) The same experiment was repeated, and samples were viewed at higher magnification at 12 hpi by using an antibody against pJ13L (bottom panels) to locate membranes in virus factories and an antibody specific for p73 (top panels) to identify virus particles. Scale bar, 4 μm .

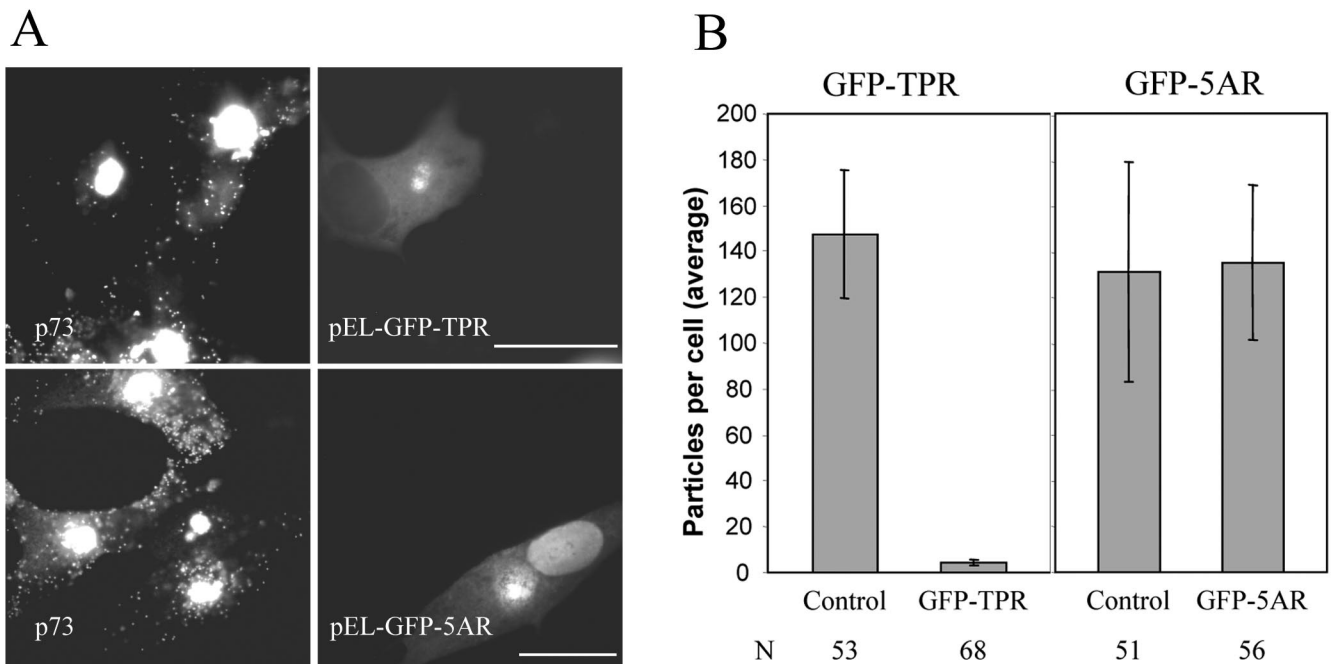


FIG. 9. Conventional kinesin is required for anterograde transport of ASFV to the cell surface. (A) Location of ASFV particles in cells expressing GFP-TPR or GFP-5AR. Vero cells were transfected with pEL-GFP-TPR or pEL-GFP-5AR as indicated. Cells were infected with ASFV 2 h later, fixed, and processed for immunofluorescence at 16 hpi. Virus particles were identified with an antibody against p73 (left panels) and the expression of GFP-TPR and GFP-5AR was monitored by the intrinsic fluorescence of GFP (right panels). Cells expressing high levels of GFP were selected. Scale bar, 20 μ m. (B) Quantification of ASFV spread to the cell periphery in cells expressing GFP-TPR or GFP-5AR. Infected cells expressing pEL-GFP-TPR or pEL-GFP-5AR were prepared as described above. The numbers of virus particles present in the cytoplasm were compared with cells (control) on the same coverslip that were infected but did not express either GFP-TPR or GFP-5AR. Results are presented as the average number of virions present in the cytoplasm per cell. Error bars indicate the standard deviation of the means. N, number of cells evaluated.

explained if the association of ASFV with the kinesin light-chain complex partially masks the epitope recognized by the kinesin antibody. In fact, the 63-90 antibody recognizes the C-terminal domain of kinesin light chain, which binds the heavy chain (21, 56, 65). Significantly, 100% of virions located outside assembly sites bound to the GFP-TPR protein, showing that ASFV was recognized as cargo by the TPR domain of kinesin light chain (Fig. 8A). This suggests that the incomplete colocalization between cytoplasmic ASFV and kinesin observed with the 63-90 antibodies is likely due to epitope masking by the ASFV-kinesin light-chain complex. Convincing evidence for use of kinesin by ASFV to leave factories came from the observation that high-level expression of the GFP-TPR protein, which binds cargo but cannot associate with microtubules, prevented ASFV anterograde transport (Fig. 9). To our knowledge this is the first evidence for the recruitment of a member of the kinesin family into a virus assembly site and subsequent use of the motor to move the virus from assembly sites to the plasma membrane.

Kinesin powers the anterograde transport of a variety of membranous and nonmembranous cellular cargoes such as mitochondria, lysosomes, ER, mRNA, and intermediate filaments (62). The disruption of conventional kinesin activity by the microinjection of antibodies specific for the light chain results in the clustering of the intermediate filament protein vimentin and mitochondria near the MTOC (25, 56, 60). Inhibition of kinesin also alters the integrity of the Golgi apparatus

(2). Significantly, ASFV infection produces a strikingly similar phenotype characterized by the clustering of mitochondria and vimentin at the MTOC and by Golgi network redistribution (26, 37, 47). It is possible that these changes in cellular architecture caused by ASFV may be bystander effects resulting from the recruitment of kinesin into virus assembly sites where it is no longer available for the transport of these cellular cargoes.

Early during ASFV infection, the GFP-TPR signal was distributed throughout the cytoplasm but was recruited into the factory when the capsid protein p73 was expressed (Fig. 8A). These observations suggest that a late signal is required for the recruitment of kinesin to viral assembly sites. The addition of nocodazole at 12 hpi greatly increased the numbers of fully assembled ASFV particles in factories 4 h later (Fig. 4B), suggesting that fully assembled viruses were preferentially recognized by kinesin for exit along microtubules. Relatively little is known about how conventional kinesin recognizes cellular cargoes and how these interactions are regulated (30). ASFV is recognized as a cargo by the TPR domains of kinesin light chain and in this way resembles cellular cargoes such as vaccinia IEV (45), the amyloid precursor protein (29), the Jun-N-terminal kinase-interacting proteins (66), and their *Drosophila* homologue, Sunday driver (9). Both the Jun-N-terminal kinase-interacting proteins (9, 11, 66) and amyloid precursor protein (29) have been proposed to mediate kinesin-dependent transport via the TPR domain of the light chain in axons.

Even though their role in nonneuronal cells needs to be established, it would be interesting to see if these proteins are recruited into ASFV assembly sites. The integral ER membrane protein kinectin is also a cellular receptor for kinesin (33). Kinectin would be a good candidate to mediate the interaction between ASFV and kinesin since ASFV particles are wrapped by ER membranes (4, 14, 15, 49). However, kinectin interacts with the kinesin heavy chain (40), which is not consistent with our observations that ASFV recruits the motor via the TPR domain of the light chain (Fig. 8). It is therefore unlikely at this point that the interaction of ASFV with kinesin is mediated by kinectin. A direct interaction between ASFV structural proteins and kinesin light chain is also possible. One candidate is the late viral protein pE120R which plays an important role in ASFV anterograde transport (5). This protein is recruited into factories, where it binds to the outer surface of virions, a position where it would have access to kinesin light chain. Most significantly, virus movement from factories is blocked if the E120R gene is disrupted, suggesting that pE120R could play a regulatory role in ASFV transport. Such a regulatory signal would be essential to prevent the exit of assembly intermediates from the factories and in this way ensure that these intermediates do not move away from the supply of structural components before assembly is completed.

How do these results for ASFV relate to the use of kinesin by other viruses? Conventional kinesin is involved in the movement of VV, but unlike ASFV, VV factories are not detected by immunostaining for kinesin and do not recruit TRP-GFP protein (45). The results suggest that conventional kinesin is not recruited into vaccinia factories and that IMVs present in factories are not recognized as cargo by kinesin light chain. Interestingly, movement of the IMV from the factory to the TGN is dependent on microtubules (51) and may, therefore, involve other members of the kinesin family. Recruitment of conventional kinesin by VV has, however, been shown to occur after envelopment by the TGN, where recruitment of kinesin allows the transport of IEV particles to the plasma membrane (45). The mechanism by which IEV recruits conventional kinesin remains to be established but appears to involve at least two viral proteins, A36R and F12L (45, 64). The movement of both IEV and ASFV to the plasma membrane is inhibited when the TPR domain of kinesin light chain is overexpressed, suggesting that conventional kinesin is the only motor involved in the anterograde transport of these virions (45) (Fig. 9). The bidirectional movement of HSV-1 observed in neurons makes it highly likely that both plus- and minus-end microtubule motors are used by viral particles (53). Indeed, immunoelectron microscopy studies have shown conventional kinesin on the surface of unenveloped HSV-1 in human fetal axons (17). In contrast to IEV and ASFV, it remains to be established whether conventional kinesin is the only motor responsible for HSV anterograde transport or whether multiple kinesin motors are involved. In fact, *in vitro* binding assays have shown that the HSV-1 tegument protein US11 can associate with the conventional kinesin heavy chain as well as with the kinesin light-chain-related protein PAT1 (7, 17). Kinesin may also be important for the transport of retroviral components since the C terminus of KIF-4, a member of the kinesin family, has been found to interact with retroviral Gag proteins in yeast two-hybrid screens (31, 61). Therefore, kinesin motors are emerg-

ing as common transporters for viruses to reach their site of budding during egress.

ACKNOWLEDGMENTS

We thank Vikki Allan (Manchester University, Manchester, United Kingdom) for discussions about motor proteins, Scott Brady (University of Texas, Dallas) for generously providing the kinesin light-chain antibody 63-90, and Manuel Borca (Plum Island Animal Disease Center, New York) for the expression vector pET-5AR. We also thank Miriam Windsor and Pippa Hawes for technical help, Sharon Brookes for the production of the SB11 antibody, Brendan Murphy (Imperial College, London) for technical advice, and Steven Archibald (IAH, Surrey, United Kingdom) and Kyle Miller (Cancer Research UK) for help with graphics and critical reading of the manuscript.

This work was supported by the BBSRC.

REFERENCES

- Afonso, C. L., C. Alcaraz, A. Brun, M. D. Sussman, D. V. Onisk, J. M. Escribano, and D. L. Rock. 1992. Characterization of p30, a highly antigenic membrane and secreted protein of African swine fever virus. *Virology* **189**: 368–373.
- Allan, V. J., H. M. Thompson, and M. A. McNiven. 2002. Motoring around the Golgi. *Nat. Cell Biol.* **4**:E236–E242.
- Alonso, C., J. Miskin, B. Hernaez, P. Fernandez-Zapatero, L. Soto, C. Canto, I. Rodriguez-Crespo, L. Dixon, and J. M. Escribano. 2001. African swine fever virus protein p54 interacts with the microtubular motor complex through direct binding to light-chain dynein. *J. Virol.* **75**:9819–9827.
- Andres, G., R. Garcia-Escudero, C. Simon-Mateo, and E. Vinuela. 1998. African swine fever virus is enveloped by a two-membraned collapsed cisterna derived from the endoplasmic reticulum. *J. Virol.* **72**:8988–9001.
- Andres, G., R. Garcia-Escudero, E. Vinuela, M. L. Salas, and J. M. Rodriguez. 2001. African swine fever virus structural protein pE120R is essential for virus transport from assembly sites to plasma membrane but not for infectivity. *J. Virol.* **75**:6758–6768.
- Arzuza, O., A. Urzainqui, J. R. Diaz-Ruiz, and E. Tabares. 1992. Morphogenesis of African swine fever virus in monkey kidney cells after reversible inhibition of replication by cycloheximide. *Arch. Virol.* **124**:343–354.
- Benboudjema, L., M. Mulvey, Y. Gao, S. W. Pimplikar, and I. Mohr. 2003. Association of the herpes simplex virus type 1 Us11 gene product with the cellular kinesin light-chain-related protein PAT1 results in the redistribution of both polypeptides. *J. Virol.* **77**:9192–9203.
- Borca, M. V., P. M. Irusta, G. F. Kutish, C. Carillo, C. L. Afonso, A. T. Burrage, J. G. Neilan, and D. L. Rock. 1996. A structural DNA binding protein of African swine fever virus with similarity to bacterial histone-like proteins. *Arch. Virol.* **141**:301–313.
- Bowman, A. B., A. Kamal, B. W. Ritchings, A. V. Philp, M. McGrail, J. G. Gindhart, and L. S. Goldstein. 2000. Kinesin-dependent axonal transport is mediated by the Sunday driver (SYD) protein. *Cell* **103**:583–594.
- Burkhardt, J. K., C. J. Echeverri, T. Nilsson, and R. B. Vallee. 1997. Overexpression of the dynamitin (p50) subunit of the dynactin complex disrupts dynein-dependent maintenance of membrane organelle distribution. *J. Cell Biol.* **139**:469–484.
- Byrd, D. T., M. Kawasaki, M. Walcoff, N. Hisamoto, K. Matsumoto, and Y. Jin. 2001. UNC-16, a JNK-signaling scaffold protein, regulates vesicle transport in *C. elegans*. *Neuron* **32**:787–800.
- Carrascosa, A. L., M. del Val, J. F. Santaren, and E. Vinuela. 1985. Purification and properties of African swine fever virus. *J. Virol.* **54**:337–344.
- Carvalho, Z. G., A. P. De Matos, and C. Rodrigues-Pousada. 1988. Association of African swine fever virus with the cytoskeleton. *Virus Res.* **11**:175–192.
- Cobbold, C., J. T. Whittle, and T. Wileman. 1996. Involvement of the endoplasmic reticulum in the assembly and envelopment of African swine fever virus. *J. Virol.* **70**:8382–8390.
- Cobbold, C., and T. Wileman. 1998. The major structural protein of African swine fever virus, p73, is packaged into large structures, indicative of viral capsid or matrix precursors, on the endoplasmic reticulum. *J. Virol.* **72**:5215–5223.
- de Matos, A. P., and Z. G. Carvalho. 1993. African swine fever virus interaction with microtubules. *Biol. Cell* **78**:229–234.
- Diefenbach, R. J., M. Miranda-Saksena, E. Diefenbach, D. J. Holland, R. A. Boadle, P. J. Armati, and A. L. Cunningham. 2002. Herpes simplex virus tegument protein US11 interacts with conventional kinesin heavy chain. *J. Virol.* **76**:3282–3291.
- Dohner, K., A. Wolfstein, U. Prank, C. Echeverri, D. Dujardin, R. Vallee, and B. Sodeik. 2002. Function of dynein and dynactin in herpes simplex virus capsid transport. *Mol. Biol. Cell* **13**:2795–2809.
- Elliott, G., and P. O'Hare. 1998. Herpes simplex virus type 1 tegument protein VP22 induces the stabilization and hyperacetylation of microtubules. *J. Virol.* **72**:6448–6455.

20. Frischknecht, F., V. Moreau, S. Rottger, S. Gonfloni, I. Reckmann, G. Superti-Furga, and M. Way. 1999. Actin-based motility of vaccinia virus mimics receptor tyrosine kinase signalling. *Nature* **401**:926–929.
21. Gauger, A. K., and L. S. Goldstein. 1993. The Drosophila kinesin light chain. Primary structure and interaction with kinesin heavy chain. *J. Biol. Chem.* **268**:13657–13666.
22. Gilbert, J. M., I. G. Goldberg, and T. L. Benjamin. 2003. Cell penetration and trafficking of polyomavirus. *J. Virol.* **77**:2615–2622.
23. Gindhart, J. G., Jr., and L. S. Goldstein. 1996. Tetratricopeptide repeats are present in the kinesin light chain. *Trends Biochem. Sci.* **21**:52–53.
24. Glotzer, J. B., A. I. Michou, A. Baker, M. Saltik, and M. Cotten. 2001. Microtubule-independent motility and nuclear targeting of adenoviruses with fluorescently labeled genomes. *J. Virol.* **75**:2421–2434.
25. Gyoeva, F. K., and V. I. Gelfand. 1991. Coalignment of vimentin intermediate filaments with microtubules depends on kinesin. *Nature* **353**:445–448.
26. Heath, C. M., M. Windsor, and T. Wileman. 2001. Aggresomes resemble sites specialized for virus assembly. *J. Cell Biol.* **153**:449–455.
27. Heath, C. M., M. Windsor, and T. Wileman. 2003. Membrane association facilitates the correct processing of pp220 during production of the major matrix proteins of African swine fever virus. *J. Virol.* **77**:1682–1690.
28. Hollinshead, M., G. Rodger, H. Van Eijl, M. Law, R. Hollinshead, D. J. Vaux, and G. L. Smith. 2001. Vaccinia virus utilizes microtubules for movement to the cell surface. *J. Cell Biol.* **154**:389–402.
29. Kamal, A., G. B. Stokin, Z. Yang, C. H. Xia, and L. S. Goldstein. 2000. Axonal transport of amyloid precursor protein is mediated by direct binding to the kinesin light chain subunit of kinesin-I. *Neuron* **28**:449–459.
30. Karcher, R. L., S. W. Deacon, and V. I. Gelfand. 2002. Motor-cargo interactions: the key to transport specificity. *Trends Cell Biol.* **12**:21–27.
31. Kim, W., Y. Tang, Y. Okada, T. A. Torrey, S. K. Chattopadhyay, M. Pfeiderer, F. G. Falkner, F. Dornier, W. Choi, N. Hirokawa, and H. C. Morse III. 1998. Binding of murine leukemia virus Gag polyproteins to KIF4, a microtubule-based motor protein. *J. Virol.* **72**:6898–6901.
32. Kreitzer, G., G. Liao, and G. G. Gundersen. 1999. Detyrosination of tubulin regulates the interaction of intermediate filaments with microtubules in vivo via a kinesin-dependent mechanism. *Mol. Biol. Cell* **10**:1105–1118.
33. Kumar, J., H. Yu, and M. P. Sheetz. 1995. Kinectin, an essential anchor for kinesin-driven vesicle motility. *Science* **267**:1834–1837.
34. Lanier, L. M., and L. E. Volkman. 1998. Actin binding and nucleation by *Autographa californica* M nucleopolyhedrovirus. *Virology* **243**:167–177.
35. Larcher, J. C., D. Boucher, S. Lazereg, F. Gros, and P. Denoulet. 1996. Interaction of kinesin motor domains with alpha- and beta-tubulin subunits at a tau-independent binding site. Regulation by polyglutamylation. *J. Biol. Chem.* **271**:22117–22124.
36. Liao, G., and G. G. Gundersen. 1998. Kinesin is a candidate for cross-bridging microtubules and intermediate filaments. Selective binding of kinesin to detyrosinated tubulin and vimentin. *J. Biol. Chem.* **273**:9797–9803.
37. McCrossan, M., M. Windsor, S. Ponnambalam, J. Armstrong, and T. Wileman. 2001. The *trans* Golgi network is lost from cells infected with African swine fever virus. *J. Virol.* **75**:11755–11765.
38. McDonald, D., M. A. Vodicka, G. Lucero, T. M. Svitkina, G. G. Borisy, M. Emerman, and T. J. Hope. 2002. Visualization of the intracellular behavior of HIV in living cells. *J. Cell Biol.* **159**:441–452.
39. Murti, K. G., R. Goorha, and M. Chen. 1985. Interaction of frog virus 3 with the cytoskeleton. *Curr. Top. Microbiol. Immunol.* **116**:107–131.
40. Ong, L. L., A. P. Lim, C. P. Er, S. A. Kuznetsov, and H. Yu. 2000. Kinectin-kinesin binding domains and their effects on organelle motility. *J. Biol. Chem.* **275**:32854–32860.
41. Parker, J. S., T. J. Broering, J. Kim, D. E. Higgins, and M. L. Nibert. 2002. Reovirus core protein mu2 determines the filamentous morphology of viral inclusion bodies by interacting with and stabilizing microtubules. *J. Virol.* **76**:4483–4496.
42. Piperno, G., M. LeDizet, and X. J. Chang. 1987. Microtubules containing acetylated alpha-tubulin in mammalian cells in culture. *J. Cell Biol.* **104**:289–302.
43. Ploubidou, A., V. Moreau, K. Ashman, I. Reckmann, C. Gonzalez, and M. Way. 2000. Vaccinia virus infection disrupts microtubule organization and centrosome function. *EMBO J.* **19**:3932–3944.
44. Ploubidou, A., and M. Way. 2001. Viral transport and the cytoskeleton. *Curr. Opin. Cell Biol.* **13**:97–105.
45. Rietdorf, J., A. Ploubidou, I. Reckmann, A. Holmstrom, F. Frischknecht, M. Zettl, T. Zimmermann, and M. Way. 2001. Kinesin-dependent movement on microtubules precedes actin-based motility of vaccinia virus. *Nat. Cell Biol.* **3**:992–1000.
46. Rodriguez, F., V. Ley, P. Gomez-Puertas, R. Garcia, J. F. Rodriguez, and J. M. Escribano. 1996. The structural protein p54 is essential for African swine fever virus viability. *Virus Res.* **40**:161–167.
47. Rojo, G., M. Chamorro, M. L. Salas, E. Vinuela, J. M. Cuezva, and J. Salas. 1998. Migration of mitochondria to viral assembly sites in African swine fever virus-infected cells. *J. Virol.* **72**:7583–7588.
48. Rosenbaum, J. 2000. Cytoskeleton: functions for tubulin modifications at last. *Curr. Biol.* **10**:R801–R803.
49. Rouiller, I., S. M. Brookes, A. D. Hyatt, M. Windsor, and T. Wileman. 1998. African swine fever virus is wrapped by the endoplasmic reticulum. *J. Virol.* **72**:2373–2387.
50. Salas, J., M. L. Salas, and E. Vinuela. 1999. African swine fever virus: a missing link between poxviruses and iridoviruses? p. 467–480. *In* E. Domingo, R. Webster, and J. Holland (ed.), *Origin and evolution of viruses*. Academic Press, London, United Kingdom.
51. Sanderson, C. M., M. Hollinshead, and G. L. Smith. 2000. The vaccinia virus A27L protein is needed for the microtubule-dependent transport of intracellular mature virus particles. *J. Gen. Virol.* **81**:47–58.
52. Smith, G. A., and L. W. Enquist. 2002. Break ins and break outs: viral interactions with the cytoskeleton of mammalian cells. *Annu. Rev. Cell Dev. Biol.* **18**:135–161.
53. Smith, G. A., S. P. Gross, and L. W. Enquist. 2001. Herpesviruses use bidirectional fast-axonal transport to spread in sensory neurons. *Proc. Natl. Acad. Sci. USA* **98**:3466–3470.
54. Sodeik, B. 2000. Mechanisms of viral transport in the cytoplasm. *Trends Microbiol.* **8**:465–472.
55. Sodeik, B., R. W. Doms, M. Ericsson, G. Hiller, C. E. Machamer, W. van't Hof, G. van Meer, B. Moss, and G. Griffiths. 1993. Assembly of vaccinia virus: role of the intermediate compartment between the endoplasmic reticulum and the Golgi stacks. *J. Cell Biol.* **121**:521–541.
56. Stenoien, D. L., and S. T. Brady. 1997. Immunochemical analysis of kinesin light chain function. *Mol. Biol. Cell* **8**:675–689.
57. Suikkanen, S., T. Aaltonen, M. Nevalainen, O. Valilehto, L. Lindholm, M. Vuento, and M. Vihinen-Ranta. 2003. Exploitation of microtubule cytoskeleton and dynein during parvoviral traffic toward the nucleus. *J. Virol.* **77**:10270–10279.
58. Sun, H., S. C. Jacobs, G. L. Smith, L. K. Dixon, and R. M. Parkhouse. 1995. African swine fever virus gene j13L encodes a 25–27 kDa virion protein with variable numbers of amino acid repeats. *J. Gen. Virol.* **76**:1117–1127.
59. Suomalainen, M., M. Y. Nakano, S. Keller, K. Boucke, R. P. Stidwill, and U. Greber. 1999. Microtubule-dependent plus- and minus end-directed motilities are competing processes for nuclear targeting of adenovirus. *J. Cell Biol.* **144**:657–672.
60. Tanaka, Y., Y. Kanai, Y. Okada, S. Nonaka, S. Takeda, A. Harada, and N. Hirokawa. 1998. Targeted disruption of mouse conventional kinesin heavy chain, kif5B, results in abnormal perinuclear clustering of mitochondria. *Cell* **93**:1147–1158.
61. Tang, Y., U. Winkler, E. O. Freed, T. A. Torrey, W. Kim, H. Li, S. P. Goff, and H. C. Morse III. 1999. Cellular motor protein KIF-4 associates with retroviral Gag. *J. Virol.* **73**:10508–10513.
62. Vale, R. D. 2003. The molecular motor toolbox for intracellular transport. *Cell* **112**:467–480.
63. Vale, R. D., T. S. Reese, and M. P. Sheetz. 1985. Identification of a novel force-generating protein, kinesin, involved in microtubule-based motility. *Cell* **42**:39–50.
64. van Eijl, H., M. Hollinshead, G. Rodger, W. H. Zhang, and G. L. Smith. 2002. The vaccinia virus F12L protein is associated with intracellular enveloped virus particles and is required for their egress to the cell surface. *J. Gen. Virol.* **83**:195–207.
65. Verhey, K. J., D. L. Lizotte, T. Abramson, L. Barenboim, B. J. Schnapp, and T. A. Rapoport. 1998. Light chain-dependent regulation of Kinesin's interaction with microtubules. *J. Cell Biol.* **143**:1053–1066.
66. Verhey, K. J., D. Meyer, R. Deehan, J. Blenis, B. J. Schnapp, T. A. Rapoport, and B. Margolis. 2001. Cargo of kinesin identified as JIP scaffolding proteins and associated signaling molecules. *J. Cell Biol.* **152**:959–970.
67. Ward, B. M., and B. Moss. 2001. Vaccinia virus intracellular movement is associated with microtubules and independent of actin tails. *J. Virol.* **75**:11651–11663.